ORNL/LTR-2018/527

FY–18 FCRD Milestone M3NT-18OR020202061
Steam Oxidation and Burst Testing in the Severe Accident Test Station

Approved for public release.
Distribution is unlimited.

B. A. Pint
L. A. Baldesberger

July 2018

OAK RIDGE NATIONAL LABORATORY
MANAGED BY UT-BATTELLE FOR THE US DEPARTMENT OF ENERGY

ORNL/LTR-2018/527

FY18 FCRD Milestone M3NT-18OR020202061
Steam Oxidation and Burst Testing in the Severe Accident Test Station

B. A. Pint and L. A. Baldesberger
Oak Ridge National Laboratory, Oak Ridge, TN, 37831

Introduction

Within six months of the March 2011 nuclear accident at Fukushima Daiichi, research began at Oak Ridge National Laboratory (ORNL) to simulate the high temperature steam oxidation accident conditions and identify potential accident tolerant fuel (ATF) cladding [1-14]. The ORNL laboratory equipment for steam oxidation equipment was expanded and made available to the entire ATF research community as the Severe Accident Test Station (SATS) in 2012 [5,15], including the capability to conduct the standard integral loss of coolant accident (LOCA) experiment [9]. A second SATS has now been deployed in an ORNL hot cell for handling irradiated specimens including reprocessed UO_2/Zr fuel [16]. The goal of an ATF cladding is to enhance safety margins in light water reactors (LWR) during beyond design basis accident scenarios by identifying materials with steam oxidation rates that are 100× slower than current Zr-based alloys at ≥1200°C. An alternative ATF cladding would significantly reduce the rate of heat and hydrogen generation in the core during a coolant-limited severe accident [17-19]. Thus, the steam oxidation behavior of candidate materials is a key metric in the evaluation of ATF concepts and also an important input into models [20-22]. Prior work has emphasized collecting steam oxidation and integral data on FeCrAl cladding so that the modeling uses the correct physical properties [23-26]. Traditionally, high temperature oxidation studies have included isothermal testing to measure reaction rates which then can be compiled to determine an activation energy such that oxidation can be modeled over a wide temperature range [7]. Also, because conventional coal- and nuclear-powered steam plants only operate at ≤600°C and advanced concepts envision 760°C as a peak temperature [27], the prior steam testing did not include such high temperatures as are now being considered (1000°-1700°C). In addition, since most accident scenarios include steadily increasing temperatures, more recent results have focused on "ramp" testing [6,12] and have examined the effect of varying the ramp rate or other variations in the heating schedule [24-26]. Thus, with no prior literature for comparison, some of the new steam oxidation behavior of FeCrAl and FeCr alloys has been surprising and difficult to interpret. In particular, a recurring question concerns the role of steam in these observations compared to simple oxidation in air or O_2. In addition to these fundamental issues, as more commercial material becomes available, the performance of commercially-manufactured tube material, like the C26M FeCrAl alloy inserted into Plant Hatch in February 2018, is of significant interest. This report summarizes recent work (1) to evaluate FeCrMo compositions as an alternative to FeCrAl and address some of the fundamental issues about protective Cr_2O_3 scale formation in high temperature steam and (2) report initial LOCA burst testing. Additional SATS integral and steam oxidation testing for FeCrAl is reported elsewhere [26,28].

Steam oxidation behavior of Fe-Cr-Mo alloys

In the process of down selecting an optimized FeCrAl composition as the primary ATF candidate, a wider range of Fe-Cr-X, SiC and MAX phase (e.g. Ti_2AlC) materials were evaluated using the SATS platform [1-7,11]. Recently some of the results for Fe-Cr alloys were summarized with an emphasis on comparing the reaction products formed isothermally in air and steam [11]. Figure 1 shows temperature limitations for candidate alloys identified by General Electric (GE) and evaluated in 4 h isothermal exposures in ambient steam or dry air using the SATS. One of the striking aspects was the very steep increase in temperature capability near 25%Cr and the recurring

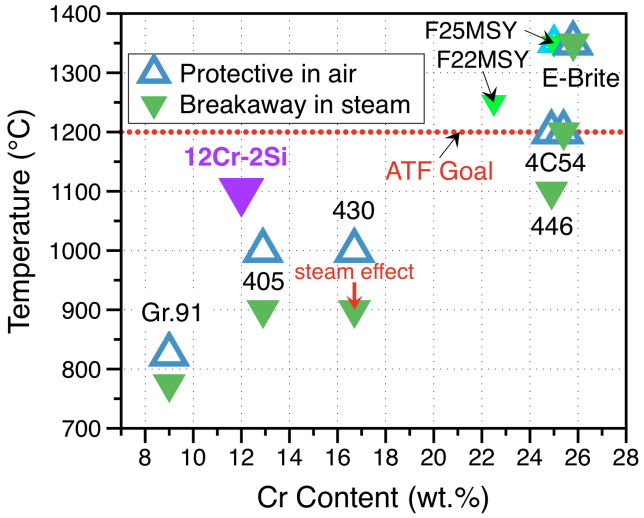

Figure 1. Steam and air temperature limits for candidate Fe-Cr alloys as a function of alloy Cr content [11]

result that steam reduced the maximum temperature capability. The maximum was defined as being able to maintain the formation of a protective Cr-rich oxide layer for 4 h in air or steam as shown below. While the commercial alloy E-Brite (Fe-26wt.%Cr-1Mo) showed promising results in steam oxidation, Cr contents over 12% are susceptible to α′ embrittlement under LWR-relevant irradiation temperature and dose regimes [17,18,29,30]. Thus, the reduction of Cr in commercial FeCrAl cladding to 12-13% compared to ~20% in many high temperature FeCrAl compositions [8].

One of the intriguing aspects of the prior work was the potential benefit of the 1%Mo addition in E-Brite. To explore the potential of replacing Cr with Mo, two laboratory alloys with 3%Mo additions and 18 and 20%Cr were cast and hot rolled for oxidation evaluations. Based on prior model alloy results and the composition of commercial alloys, 0.7%Mn, 0.25%Si and 0.1%Y additions also were included in these alloys. The measured compositions are shown in Table 1. Figure 2 shows the thermogravimetric results at 1200°C where both alloy specimens formed

Table 1. Chemical composition of relevant Fe-based alloys measured using inductively coupled plasma and combustion analyses.

Alloy	Fe	Cr	Mo	Mn	Si	Y	Other
446	73.4	24.9	0.01	0.76	0.19	<	0.2Ni,0.1Nb,0.1V,0.10N
4C54	72.5	25.4	0.02	0.71	0.49	<	0.3Ni,0.1V,0.17N,0.004S
E-Brite	72.6	25.8	1.0	<	0.22	<	0.1Ni,0.1V,0.1Nb,0.010S
11Cr-16Mo	72.5	11.2	16.2	<	0.01	<	0.05 La, 0.002S
11Cr-23Mo	66.1	10.9	23.0	<	<	<	0.05Cu, 0.02 La, 0.004S
18Cr+3Mo	77.8	18.3	2.9	0.67	0.26	0.098	0.0005 S
20Cr+3Mo	76.3	19.7	2.9	0.71	0.25	0.086	0.0004 S
25Cr+Mn,Si	74.0	25.0	<	0.67	0.25	0.002	0.0030 S
C26M	bal.	12.2	2.04	n.d.	0.20	0.04	6.1 Al,<0.01 C,<0.005 S

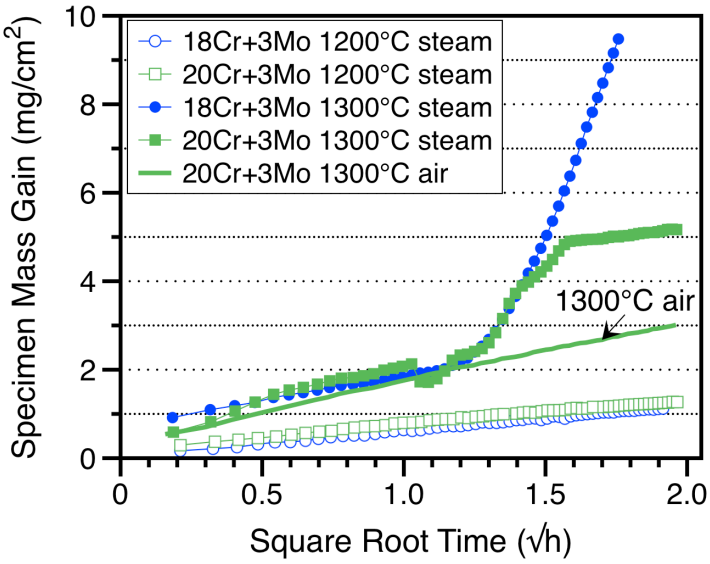

Figure 2. Specimen mass gain of Fe-Cr-Mo coupons during isothermal testing at 1200°-1300°C plotted versus the square root of time to show the parabolic relationship.

protective Cr_2O_3 scales with very similar parabolic rate constants ~$9x10^{-11}g^2/cm^4s$. At 1300°C, neither specimen was able to maintain the formation of a protective scale for 4 h in steam. The acceleration in mass gain is associated with the formation of Fe-rich oxide nodules. For the Fe-20Cr-3Mo specimen, the rate slowed again after an initial acceleration. For the Fe-18Cr-3Mo specimen, the mass gain continued to accelerate for the rest of the experiment. In contrast, Figure 2 also shows the parabolic mass gain for a 20Cr specimen exposed to air at 1300°C with a rate of $5x10^{-10}g^2/cm^4s$. These rates are much faster than those for alumina on FeCrAl alloys. They are comparable to alumina rates in steam at ~200°C higher temperature [10].

Figure 3 shows examples of the oxide scales formed on the 3%Mo alloys. Neither alloy formed an inner continuous Si-rich oxide layer at 1200°C, Figures 3a and 3b, which is consistent with similar

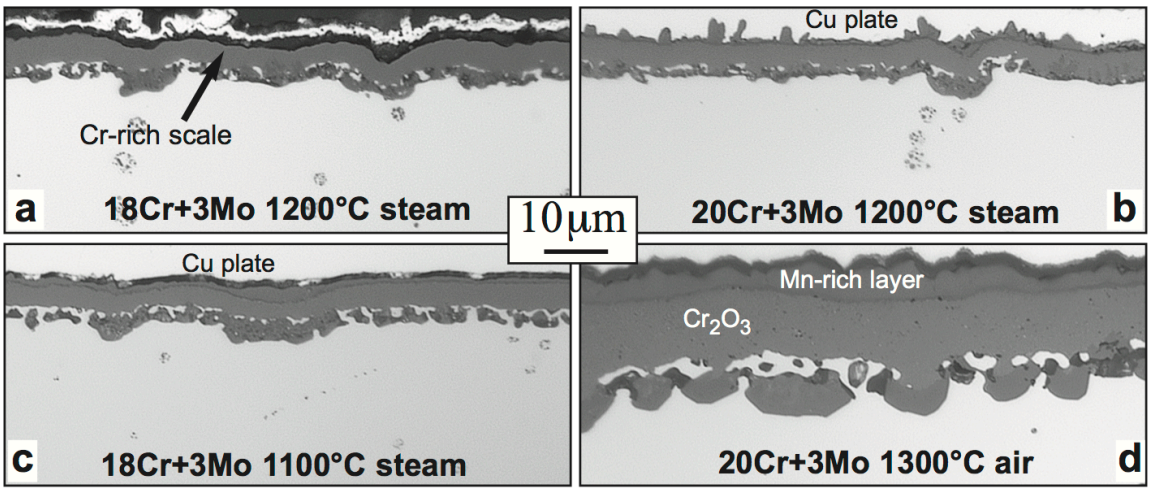

Figure 3. Light microscopy of polished sections of Fe-Cr-Mo alloys after oxidation for 4 h in (a,b) 1200°C steam, (c) 1100°C steam and (d) 1300°C air.

observations for Fe-Cr model alloys oxidized at this temperature [11]. What was unusual is that it appeared that metal was trapped between the continuous Cr-rich oxide and the discontinuous inner oxide layer. Furthermore, similar structures appeared to form at 1100°C (Figure 3c) and 1300°C (Figure 3d). For the thicker scale formed at 1300°C, a distinct outer layer likely rich in Mn was observed and was likely present in the other cases as well. Additional characterization of these scales is in progress to clearly identify the reaction products. If the metal trapped between these layers becomes depleted in Cr and begins to form voluminous Fe-rich oxide, the protective scale could be locally disrupted. Table 1 indicates that, in addition to 1%Mo, E-Brite contains no Mn and a low Si content. While Mn and Si are thought to be beneficial at lower temperatures in stainless steels, it might be interesting to understand their role at 1200°C in steam.

Two additional FeCrMo alloys were evaluated that were fabricated previously for a solid oxide fuel cell application with very high (16-23%) Mo contents to match the thermal expansion of the functional ceramic components [32]. Unfortunately, these compositions with only ~11%Cr (Table 1) performed poorly in steam at 800°C and suggest that high Mo steels are not particularly promising to significantly lower the Cr content for this application. However, these alloys contained no intentional Mn and Si additions and were not hot rolled, which may not be optimal for oxidation resistance. Figure 4 summarizes the current FeCrMo results. The 3%Mo additions showed some benefit compared to Fe-20%Cr and considerable composition space remains unexplored, particularly for compositions near Fe-15Cr-5Mo.

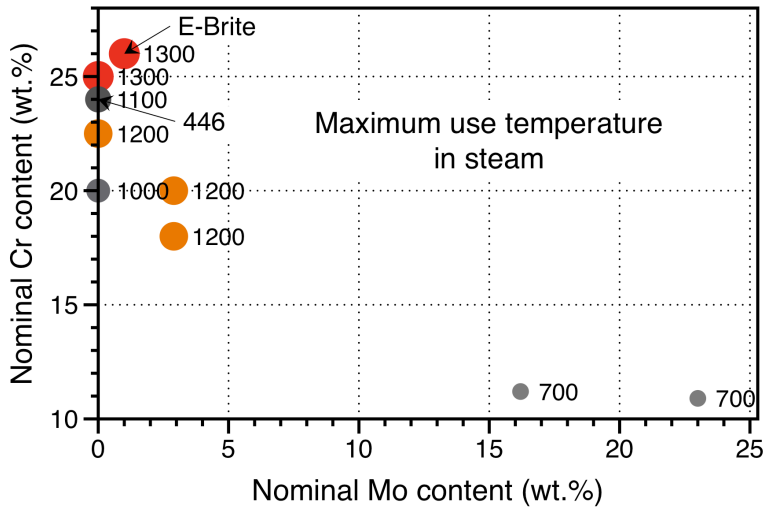

Figure 4. Composition map for Fe-Cr-Mo alloys with the maximum use temperature noted for each alloy composition.

Effect of steam on Cr_2O_3 formation

While previous work studied the effect of steam on the scale microstructure formed on Fe-Cr alloys [11], it did not address whether steam affected the parabolic rate constant or oxide thickness compared to Cr_2O_3 formed in dry oxidizing environments. The data used to generate Figure 1 was further evaluated to address this question. One issue that was encountered was that an increase in the mass gain could be attributed to Fe-rich oxide formation rather than faster Cr_2O_3 growth. Thus, it was necessary to characterize the oxide microstructure as well as calculate the rates. Examples are shown for two alloys in Figure 5 where the Arrhenius behavior for all of the Cr_2O_3-only rate constants was fit with a dashed line. In Figure 5a, alloy 446 specimens (Table 1) began to show

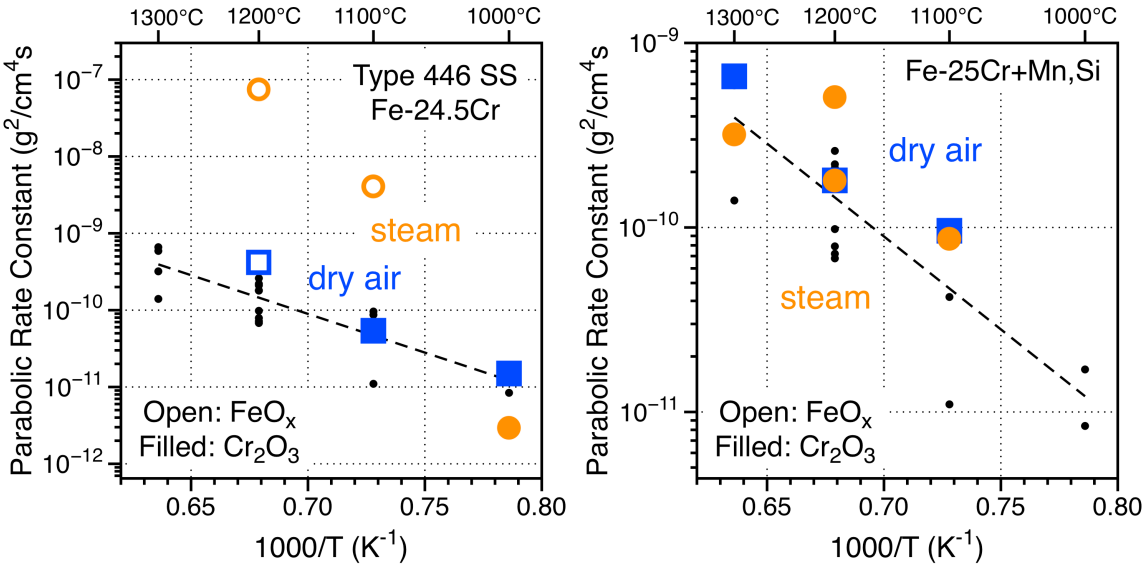

Figure 5. Arrhenius plot of parabolic rate constants measured in both dry air and steam as a function of reciprocal temperature with emphasis on results for (a) alloy 446 and (b) laboratory Fe-25Cr+Mn,Si.

Fe-rich oxide formation in steam at 1100°C and in air at 1200°C. The only comparison temperature for Cr_2O_3 growth was at 1000°C. For the model Fe-25Cr+Mn,Si specimens in Figure 5b, Cr_2O_3 formation occurred in all conditions from 1100°-1300°C. The rates were very similar in both environments and a statistical analysis would be required to determine any difference in rates between air and steam. In one case at 1200°C steam where the conditions were repeated, the two values were considerably different. The compilation of rates suggests that there is no significant difference in rate constants between experiments conducted in steam and dry air.

Figure 6 shows pairs of oxide scales formed during 4 h exposures in steam and dry air for one commercial alloy (4C54) and one model alloy (Fe-25Cr+Mn,Si). For the 4C54 specimens, oxide thickness measurements (40-100 values using image analysis of light microscopy images) are shown in box and whisker plots in Figure 7 with the median values (line in the box) noted for each condition. The significant increase in oxide thickness in steam at 1200°C was due to the formation of Fe-rich oxide. While the median oxide thickness was slightly lower at 1100°C in steam than in dry air, the result is not statistically significant given the range in values measured. Figure 8 shows four different temperature/alloy pairs that were identified where a Cr_2O_3 scale formed in both steam and dry air. In this case, the average oxide thickness and standard deviation are shown. Again, due to the scatter in values measured no significant difference could be noted in scale thickness between the two environments. Thus, there was no clear evidence in this set of experiments that steam increased or decreased the scale growth rate. The major effect of testing in steam appears to be the formation of rapidly growing Fe-rich oxides at lower temperatures compared to exposures in dry air as illustrated in Figure 1. The mechanism for this effect remains a subject of debate.

Initial LOCA burst testing of commercial C26M FeCrAl tubing

Now that significantly more commercial tubing is available, additional LOCA burst testing could be conducted, which requires ~30 cm long pieces for each experiment. Of particularly interest was the new C26M composition which was selected for insertion into Southern Nuclear's Plant Hatch

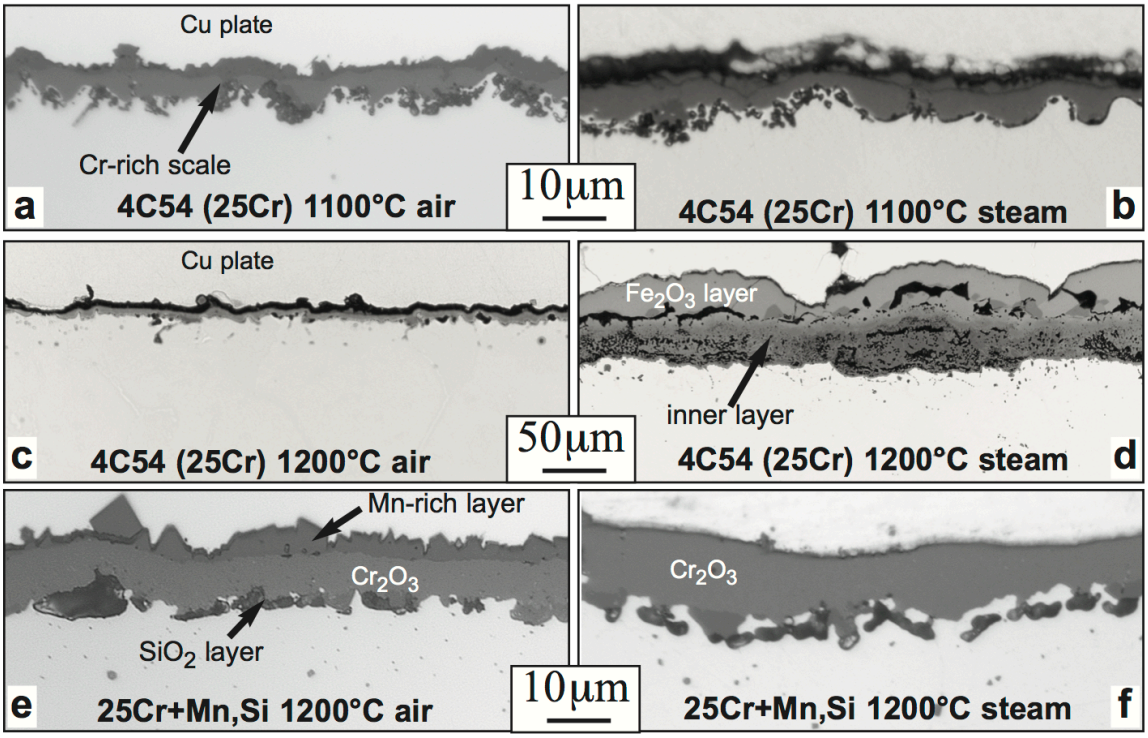

Figure 6. Light microscopy of polished sections of the thermally grown oxide formed after 4h (a) alloy 4C54 1100°C air, (b) alloy 4C54 1100°C steam, (c) alloy 4C54 1200°C air, (d) alloy 4C54 1200°C steam (e) Fe-25Cr,1200°C air and (f) Fe-25Cr,1200°C steam.

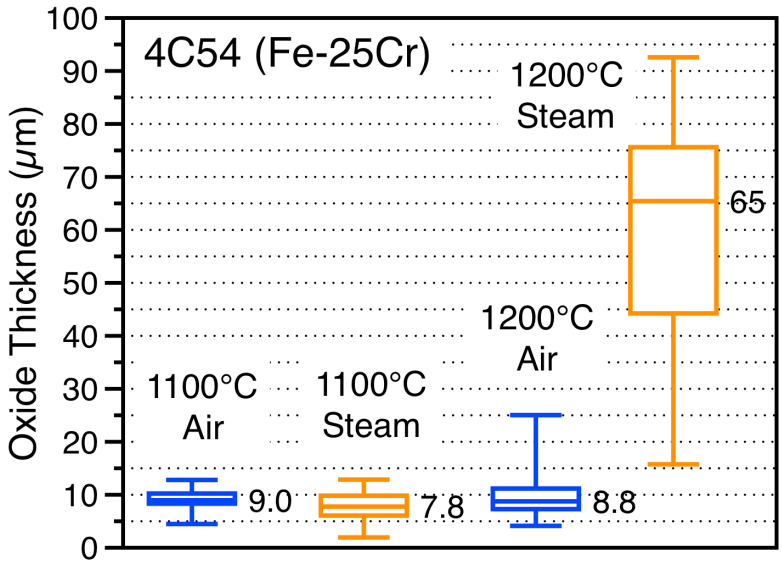

Figure 7. Box and whisker plots of oxide thickness measurements for scales formed on 4C54 specimens after 4 h isothermal exposures in four different conditions. The box shows the 25 and 75% values and the whisker denote the minimum and maximum measured thicknesses. The median values in each case are noted with a line in the box.

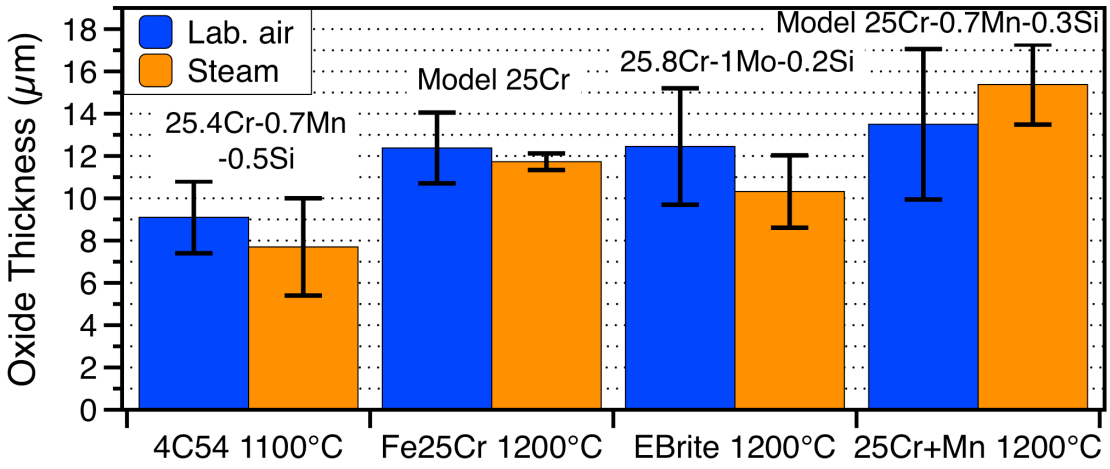

Figure 8. Average oxide thickness values for similar 4 h exposures in steam and dry air for several different alloys.

in February 2018. Figure 9 shows the initial burst data from the first two batches of material compared to prior data points obtained in the SATS [9]. The C26M composition included Mo and Si additions (Table 1) for higher tensile properties compared to the first generation of FeCrAlY alloys, such as those designated B135Y (13Cr-5Al) and B154Y (15Cr-4Al) in Figure 9. The first batch of C26M specimens did not show improved burst temperatures compared to the 1st generation results and this was attributed to issues with the processing that were resolved in the second batch of material. Figure 9 shows an increase in the burst temperature for the 2nd batch of material. As an initial assessment of the crack location and size at burst, Figure 10 shows preliminary results.

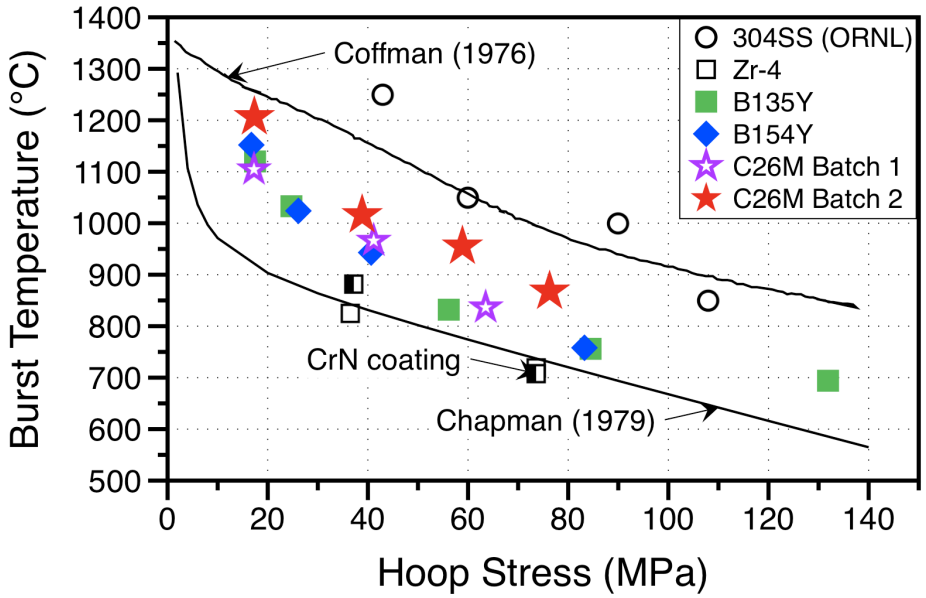

Figure 9. Burst temperature as a function of engineering hoop stress for various cladding materials examined in the SATS (data points [9]) alongside empirical correlations (lines) from the literature for Zr-alloys [33] and 304SS [34]

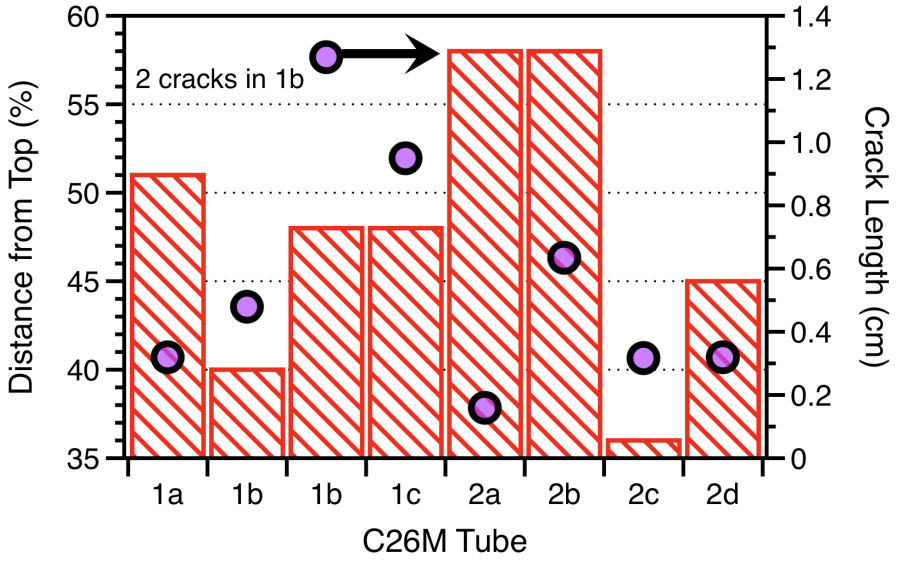

Figure 10. Location and length of the cracks formed in the C26M burst tubes. The specimens from batches 1 and 2 are listed in order of increasing hoop stress in Figure 9.

All of the cracks were relatively small, particularly for the second batch of material. Higher pressure tests are needed to evaluate this effect across the range previously evaluated for the weaker first generation FeCrAlY tubes [9].

Summary

Since 2011, the high temperature steam oxidation resistance of many different candidate ATF cladding materials has been evaluated in the ORNL SATS. Coupons of new FeCrMo compositions were evaluated, however, the Cr contents are still relatively high (18-20%) and the maximum use temperature was limited to ~1200°C in steam testing. A review of prior commercial and laboratory alloys could not identify a statistically significant effect of steam on the growth rate or oxide thickness of Cr_2O_3 scales compared to those formed in dry air. Initial burst testing of commercial 2nd generation FeCrAl (C26M) tubes was conducted. For the second batch of C26M material processed under more optimal conditions, an increase in the burst temperature was noted compared to the first batch of C26M and previous 1st generation FeCrAl tube results. Initial characterization showed relatively small crack sizes for experiments up to 76 MPa hoop stresses. Additional testing with higher stresses is in progress and will be reported in a future report [28].

Acknowledgments

The experimental work was conducted by M. Howell, T. Lowe and T. Jordan. S. S. Raiman and S. Dryepondt provided useful comments on the manuscript. This research was funded by the U.S. Department of Energy's Office of Nuclear Energy, Advanced Fuel Campaign of the Fuel Cycle R&D program.

References

[1] T. Cheng, J. R. Keiser, M. P. Brady, K. A. Terrani and B. A. Pint, "Oxidation of fuel cladding candidate materials in steam environments at high temperature and pressure," *J. Nucl. Mater*. 427 (2012) 396-400.

[2] B. A. Pint, K. A. Terrani, M. P. Brady, T. Cheng and J. R. Keiser, "High Temperature Oxidation of Fuel Cladding Candidate Materials in Steam-Hydrogen Environments," *J. Nucl. Mater*. 440 (2013) 420-427.

[3] B. A. Pint, K. A. Terrani, J. R. Keiser, M. P. Brady, Y. Yamamoto and L. L. Snead, "Material Selection for Fuel Cladding Resistant to Severe Accident Scenarios," NACE Paper ED2013-3083, Houston, TX, presented at the 16th Environmental Degradation conference, Asheville, NC, August 2013.

[4] K. A. Terrani, C. M. Parish, D. Shin and B. A. Pint, "Protection of zirconium by alumina- and chromia-forming iron alloys under high-temperature steam exposure," *J. Nucl. Mater*. 438 (2013) 64-71.

[5] K. A. Terrani, B. A. Pint, C. M. Parish, C. M. Silva, L. L. Snead and Y. Katoh, "Silicon Carbide Oxidation in Steam up to 2 MPa," *J. Am. Ceram. Soc.* 97 (2014) 2331-2352.

[6] B. A. Pint, K. A. Unocic and K. A. Terrani, "The Effect of Steam on the High Temperature Oxidation Behavior of Alumina-Forming Alloys," *Mater. High Temp*. 32 (2015) 28-35.

[7] B. A. Pint, K. A. Terrani, Y. Yamamoto and L. L. Snead, "Material Selection for Accident Tolerant Fuel Cladding," *Met. Mater. Trans.* 2E (2015) 190-196.

[8] Y. Yamamoto, B. A. Pint, K. A. Terrani, K. G. Field, Y. Yang and L.L. Snead, "Development and Property Evaluation of Nuclear Grade Wrought FeCrAl Fuel Cladding for Light Water Reactors," *J. Nucl. Mater*. 467 (2015) 703-716.

[9] C. P. Massey, K. A. Terrani, S. N. Dryepondt and B. A. Pint, "Cladding burst behavior of Fe-based alloys under LOCA," *J. Nucl. Mater*. 470 (2016) 128-138.

[10] K. A. Unocic, Y. Yamamoto and B. A. Pint, "Effect of Al and Cr Content on Air and Steam Oxidation of FeCrAl Alloys and Commercial APMT Alloy," *Oxid. Met.* 87 (2017) 431–441.

[11] B. A. Pint and K. A. Unocic, "Evaluation of Fe-Cr Alloys for Accident Tolerant Fuel Cladding," *Oxid. Met.* 87 (2017) 515-526.

[12] B. A. Pint, "Performance of FeCrAl for Accident Tolerant Fuel Cladding in High Temperature Steam," *Corros. Rev.* 35(3) (2017) 167-175.

[13] K. G. Field, Y. Yamamoto, B. A. Pint, M. N. Gussev and K. A. Terrani, "Accident Tolerant FeCrAl Fuel Cladding: Current Status Towards Commercialization, in *Proceedings of the 18th International Conference on Environmental Degradation of Materials in Nuclear Power Systems–Water Reactors*, J.H. Jackson et al. (eds.), TMS, Warrendale, PA, pp.165-173.

[14] B. A. Pint, K. A. Terrani and R. B. Rebak, "Steam Oxidation Behavior of FeCrAl Cladding," in *Proceedings of the 18th International Conference on Environmental Degradation of Materials in Nuclear Power Systems–Water Reactors*, J.H. Jackson et al. (eds.), TMS, Warrendale, PA, pp.235-244.

[15] M. Snead, Y. Yan, M. Howell, J. Keiser and K. Terrani, "Severe Accident Test Station Design Report," ORNL Report TM-2015/556, Oak Ridge, TN, 2015.

[16] A. M. Raftery, Y. Yan, T. S. Smith, Z. M. Burns, K. A. Terrani and K. D. Linton, "In-cell Re-fabrication and Loss-of-coolant Accident (LOCA) Testing of High Burnup Commercial Spent Fuel," ORNL/TM-2018/891

[17] S. J. Zinkle, K. A. Terrani, J. C. Gehin, L. J. Ott and L. L. Snead, "Accident tolerant fuels for LWRs: A perspective," *J. Nucl. Mater*. 448 (2014) 374-379.

[18] K. A. Terrani, S. J. Zinkle and L. L. Snead, "Advanced Oxidation-Resistant Iron-Based Alloys for LWR Fuel Cladding," *J. Nucl. Mater*. 448 (2014) 420-435.

[19] K. A. Terrani, "Accident tolerant fuel cladding development: Promise, status, and challenges," *J. Nucl. Mater.* 501 (2018) 13–30.
[20] K. Vierow, Y. Liao, J. Johnson, M. Kenton and R. Gauntt, "Severe accident analysis of a PWR station blackout with the MELCOR, MAAP4 and SCDAP/RELAP5 codes, Nucl. Eng. Design 234 (2004) 129-145.
[21] L. J. Ott, K. R. Robb and D. Wang, "Preliminary assessment of accident-tolerant fuels on LWR performance during normal operation and under DB and BDB accident conditions," J. Nucl. Mater. 448 (2014) 520-533.
[22] K. R. Robb, M.W. Francis and L. J. Ott, "Insight from Fukushima Daiichi Unit 3 Investigations Using MELCOR," Nuclear Technology, 186 (2014) 145-160.
[23] B. A. Pint and J. W. McMurray, "Steam Oxidation Testing in the Severe Accident Test Station (SATS)," ORNL/LTR-2016/425, Oak Ridge, TN, 2016.
[24] B. A. Pint, "Steam Oxidation Testing in the Severe Accident Test Station," ORNL/LTR-2017/368, Oak Ridge, TN, 2017.
[25] K. R. Robb, M. Howell and L. J. Ott, "Parametric and experimentally informed BWR Severe Accident Analysis Utilizing FeCrAl," ORNL TM-2017/373, Oak Ridge, TN, 2017.
[26] K. R. Robb, M. Howell and L. J. Ott, "Design and analysis of oxidation tests to inform FeCrAl ATF severe accident models," ORNL/SPR-2018/893, Oak Ridge, TN, 2018.
[27] R. Viswanathan, J. Shingledecker and R. Purgert, "Evaluating Materials Technology for Advanced Ultrasupercritical Coal-Fired Plants," *Power*, *154*(8) (2010) 41-45.
[28] B. A. Pint, "Steam Oxidation, Burst and Critical Heat Flux Testing of Commercial FeCrAl Fuel Cladding," ORNL/LTR-2018/530, Oak Ridge, TN, 2018.
[29] K. G. Field, X. Hu, K. Littrell, Y. Yamamoto and L. L. Snead, "Radiation Tolerance of Neutron-Irradiated Model Fe-Cr-Al Alloys," J. Nucl. Mater. 465 (2015) 746-755.
[30] P. D. Edmondson, S. A. Briggs, Y. Yamamoto, R. H. Howard, K. Sridharan, K. A. Terrani, K. G. Field, "Irradiation-enhanced α′ precipitation in model FeCrAl alloys," Scripta Materialia 116 (2016) 112–116.
[31] B. A. Pint, R. Peraldi and P. J. Maziasz, "The Use of Model Alloys to Develop Corrosion-Resistant Stainless Steels," Mater. Sci. Forum, 461-464, 815-822 (2004).
[32] B. A. Pint, B. L. Armstrong, I. G. Wright, M. P. Brady, P. F. Tortorelli, R. R. Judkins and T. R. Armstrong, "Ferritic Alloy Compositions," U.S. patent application 2009/0286107, Nov. 19, 2009.
[33] R. H. Chapman, Multirod Burst Test Program, Progress Report for April-June 1979, US NRC Report NUREG/CR-1023, November 1979, Oak Ridge National Laboratory, 1979.
[34] F. D. Coffman, "LOCA Temperature Criterion for Stainless Steel Clad Fuel," US NRC Report NUREG-0065, 1976.